CO5-1

Volcanic and Tectonic History of Philippine Sea Plate (South of Japan) Revealed by $^{40}Ar/^{39}Ar$ Dating Technique

O. Ishizuka[1], H. Yoshino[2], H. Yoshinaga[2], Y. Iinuma[2], R. Okumura[2], T. Fujii[3]

[1] *Geological Survey of Japan, AIST*
[2] *Institute for Integrated Radiation and Nuclear Science, Kyoto University*
[3] *Graduate School of Engineering, Osaka University*

INTRODUCTION: The West Philippine Basin (WPB) occupies the western half of the modern Philippine Sea Plate. However, its origin, spreading history and tectonic relationship to the adjacent Izu-Bonin-Mariana arc remains poorly understood (e.g., Ishizuka et al., 2011). In particular, the disposition of the WPB spreading in relation to the nascent Izu-Bonin-Mariana arc is critical in reconstructions of Philippine Sea plate tectonics which, in turn, have ramifications for the subduction initiation of the Pacific Plate.

EXPERIMENTS: Ages of 25 volcanic rock samples were determined using the $^{40}Ar/^{39}Ar$ dating facility at the Geological Survey of Japan/AIST. Details of the procedures are reported in Ishizuka et al. (2018). 5-15 mg of phenocryst-free groundmass, crushed and sieved to 180 – 250 μm in size, was analyzed using a stepwise heating procedure. The samples were treated in 6N HCl for 30 minutes at 95°C with stirring to remove any alteration products present in groundmass and interstitial spaces. The samples were further treated with 6N HNO_3 for 30 minutes at 95°C with stirring. After this treatment, samples were examined under a microscope. Sample irradiation was done at the Kyoto University Reactor (KUR). At the KUR, the neutron irradiation was performed for 10 h at the hydro-irradiation port under 1 MW operation, where thermal and fast neutron fluxes are 1.6 x 10^{13} and 7.8 x 10^{12} n/ cm^2 s, respectively. Argon isotopes were measured in a peak-jumping mode on an IsotopX NGX noble gas mass spectrometer fitted with a Hamamatsu Photonics R4146 secondary electron multiplier.

RESULTS: We investigated the intersection of a spreading center with an island arc within the WPB, i.e. an arc-ridge-arc triple junction, using a combination of submersible sampling and shipboard geophysics. We use Ar-Ar dating, elemental concentrations and Sr-Nd-Pb radiogenic isotope ratios to constrain the structure, age and origin of magmatism as spreading interacted with the arc.

Between 33-31 Ma the tip of the WPB spreading center was in the back-arc west of the Kyushu-Palau Ridge (KPR) arc. Spreading volcanism had mantle-like Ce/Pb and Th/Ce indicating a lack of slab flux. Radiogenic isotopes form a trajectory towards an EM-2-like mantle component.

The final stage of spreading/rifting-related activity occurred between 31-28.5 Ma when the spreading axis rotated from NW-SE to E-W and propagated eastwards into the arc, and directly intersect the KPR. This caused rifting and overlapping MORB-like magmatism on the frontal line of the KPR arc. During the final stage magmatism La/Sm and Nb/Zr increased while Pb and Sr isotopes became progressively more radiogenic, demonstrating a progressive decrease in the degree of partial melting and preferential tapping of the EM-2 component. This change in melt generation and composition appears a common process at the end of spreading.

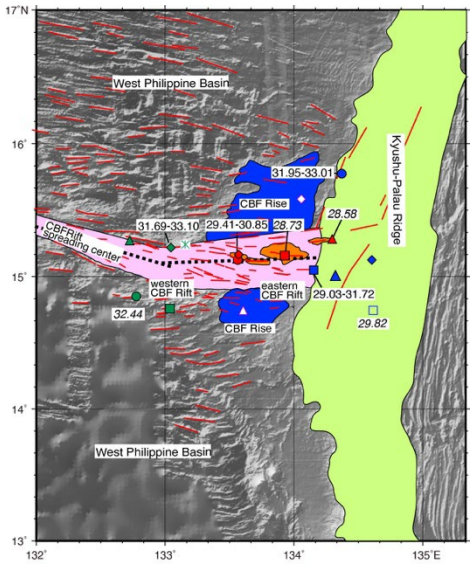

Fig. 1. Geological interpretation of the CBF Rift-KPR intersection area with $^{40}Ar/^{39}Ar$ age data (shown in Ma) on the recovered basalt at each station (Ishizuka et al., 2026). The data is based on results of this study and a previous study (ages shown in Italics are from Ishizuka et al.,

REFERENCES:

[1] O. Ishizuka *et al.*, Geochem. Geophys. Geosyst. 12 (2011), Q05005.
[2] O. Ishizuka *et al.*, Chem. Geol., 703, (2026) 123232.

CO5-2

Evaluation of water solubility in Mg_2SiO_4 olivine under high pressure

N. Tomioka[1], T. Watanabe[2], T. Kawazoe[2], T. Inoue[2], K. Shimizu[1], T. Ushikubo[1], H. Arima-Osonoi[3], Y. Umeda[3], C. Umehara[3] , T. Okuchi[3]

[1]*Kochi Institute for Core Sample Research, Japan Agency for Marine-Earth Science and Technology*
[2]*Graduate School of Advanced Science and Engineering, Hiroshima University*
[3]*Institute for Integrated Radiation and Nuclear Science, Kyoto University*

INTRODUCTION: Water was delivered to the early Earth by hydrated planetesimals. During the subsequent magma ocean stage of the Earth, water was partitioned among major reservoirs; some was incorporated into iron in the core and into silicate minerals in the mantle [1, 2]. Understanding the link between early Earth evolution and its water budget requires evaluating hydrogen storage in the silicate mineral structures. Olivine (Mg_2SiO_4), the dominant mineral in the upper mantle (<400 km depth), still lacks reliable estimates of its water content. This is due to (i) limited hydrogen incorporation into its crystal structure, (ii) possible submicron hydrous inclusions, and (iii) the need for microscale analytical techniques to determine water content while avoiding such inclusions. In this study, we develop a method to evaluate hydrogen incorporation in olivine synthesized under high-pressure and high-temperature conditions using integrated microanalytical techniques.

EXPERIMENTS: In the synthesis experiments, powders of $Mg(OH)_2$, MgO, and SiO_2 were mixed as starting materials, sealed in an Au–Pd capsule, and placed in a cell assembly. The samples were held at 11.4 GPa and 1250 °C for 30 minutes using a multi-anvil apparatus to synthesize hydrous olivine. The recovered samples were analyzed using secondary ion mass spectrometry (SIMS) to precisely determine the water content as OH groups incorporated into the olivine structure. In addition, a portion of each sample was prepared as an ultrathin section (~100 nm thick) using a focused ion beam (FIB) system and examined by transmission electron microscopy (TEM) for microstructural observation. Furthermore, the same sample was analyzed by the micro-focused X-ray diffractometer (μXRD; Rigaku SmartLab 9kW) at KURNS, Kyoto Univ.

RESULTS: Olivine occurs as grains smaller than ~150 μm, coexisting with clinoenstatite ($MgSiO_3$) and quench crystals derived from the melt. The H_2O content of hydrous olivine, determined by SIMS, is 3900±500 ppm. Preliminary μXRD measurements obtained from regions ~100 μm in diameter confirm that the unit cell of hydrous olivine is slightly expanded compared to that of anhydrous olivine (Fig. 1). Transmission electron micrographs and electron diffraction patterns from the olivine grain with the highest water content (4800 ppm) show no evidence of hydrous defects or inclusions, even at the nanoscale (Fig. 2). These results demonstrate that up to ~4000 ppm H_2O can be homogeneously incorporated directly into the olivine structure as hydroxyl groups. They also raise the possibility that previously reported water contents in olivine (8500–8900 ppm), based solely on FTIR measurements [3] for samples synthesized under similar pressure–temperature conditions, may have been overestimated, although more systematic investigation is required.

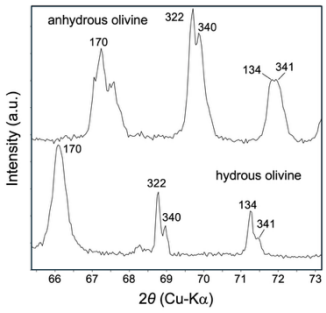

Fig. 1. XRD patterns of anhydrous and hydrous olivine.

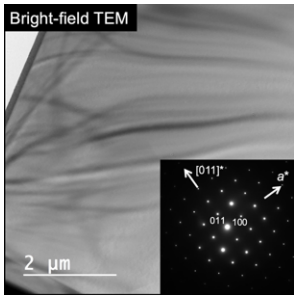

Fig. 2. TEM image and electron diffraction pattern of a hydrous olivine crystal.

REFERENCES:

[1] S. Karato, Earth Planet. Sci. Lett., **301** (2011) 413.
[2] T. Okuchi, Science, **278** (1997) 1781.
[3] J. R. Smyth *et al.*, Geophys. Res. Lett., **33** (2006) L153011.

CO5-3

Size Distribution and Long-term Concentration Change of Constituent Elements in the Atmospheric Aerosols Observed at Sakai, Osaka

Norio Ito[1], Hisao Yoshinaga[2]

[1] *Radiation Research Center, Osaka Metropolitan University*

[2] *Institute for Integrated Radiation and Nuclear Science, Kyoto University*

The atmospheric aerosols which are particles suspended in the atmosphere with wide range of particle size, 10nm ～100 μm, affect our health and the climate. Element constituents in the atmospheric aerosols have the different concentrations on the particle sizes. By the difference of concentration in elements on the particle size, the effect of particles on our health and the climate change by its size distribution. To estimate source contribution from the natural sources such as the soil and sea spray, artificial sources such as fuel burning, emission from industries and the effect of atmospheric aerosol to our health, we have observed the atmospheric aerosols in different size rages (9 size rages)at Sakai, Osaka since 1995. Usually the size distribution of elements have two peaks, referring to V and Sb in Fig.1, that are found in 0.2 ～1.0μm as fine particle element and found in 2～5μm as coarse particle element. So, the difference of the effect from the coarse particle element and fine particle element are needed to recognize. In this report we show the result of size distribution of analyzed elements and mean concentration and mean size for the elements in the samples analyzed by neutron activate analysis.

The aerosols samples have been collected on polyethylene sheet using Andersen sampler with 9 particle size ranges (<0.43,0.43～0.65,0.65～1.1,1.1～2.1,2.1～3.3,3.3～4.7,4.7～7.0,7.0～11,>11μm) on one week sampling time. The elements in some of the samples were analyzed by neutron activation analysis using Kyoto University nuclear reactor. We got the size distribution of 23 elements (Al,,Ba,Br,Ca,Ce,Cl,Cr,Cs,Fe,K,La,Mn,Mo,Na,Sb,Sc,Sm,Th,Ti,V,Zn),and got the mean concentration and mean size (Fig.1).

From this results, we have classified the size distribution into three type of size distribution, (1) distributed mainly in the coarse particle, mainly contributed from natural sources such as soil and sea salt:Al, Ba,Ca, Ce,Cr, Fe,Na,Sc,Sm,Th,Ti (2) distributed mainly in the fine particles contributed mainly from the source on burning and the secodary products from gaseous matters:As, Br, Cs ,V(3) distributed in both coarse and fine particles, K, Mo,Sb, Zn Mo.

Also we got the long−term trend(1995-2024) of element concentration in fine and coarse particles. Result of relative (ratio to mean concentration) increase rate for the element in the coarse and fine particles are shown on Fig.2. From this trend , almost of the elements in the fine particles have the decrease trend . This decrease trend might be caused by the fuel and emission control of the industry , incinerator and vehicle by the government . Cl, Sb,V have the clear decrease trend(more than 4% decrease per year).

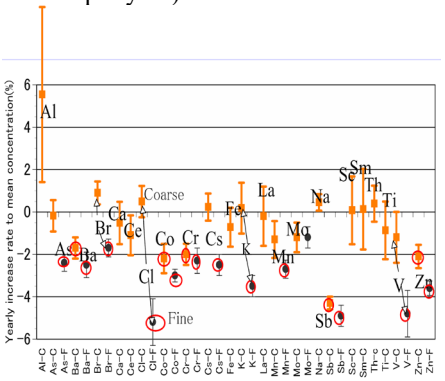

Fig.2 Relative (ratio to mean concentration) increase rate of element in the coarse and fine particles

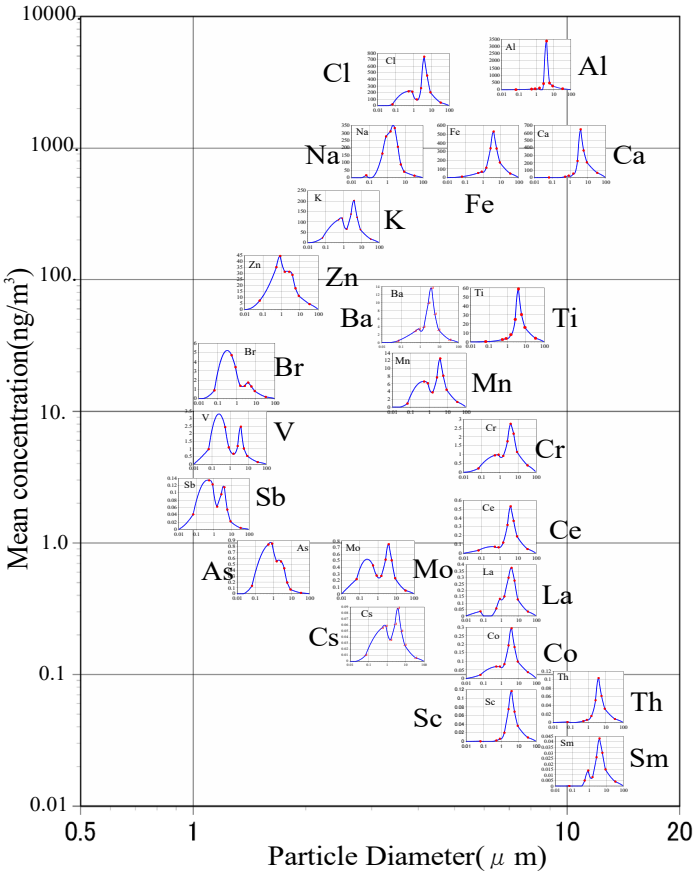

Fig.1 Size distributions of element in the atmospheric aerosols observed at Sakai,Osaka. Each size distribution is located at the position made by mean concentration and mean size for each element.

CO5-4

Laboratory-based analysis of synthetic high-density minerals of ≤100 μm crystal sizes using microfocused X-ray beam I

T. Okuchi[1], N. Tomioka[2], H. Arima-Osonoi[1], Y. Umeda[1]

[1]*Institute for Integrated Radiation and Nuclear Science, Kyoto University*
[2]*Kochi Institute for Core Sample Research, Japan Agency for Marine-Earth Science and Technology*

INTRODUCTION: Planet Earth is also known as the Water Planet. Throughout its 4.6 billion years of evolution history, liquid water covered a major part of Earth's surface and played a crucial role. On the other hand, by recent planetary exploration studies in the inner solar system, it was confirmed that solid materials occurring around Earth had contained a large amount of hydrogen equivalent to orders of magnitude more water than that currently exists on Earth. In other words, the Water Planet now seems not to be particularly rich in water. Thus, it is important to pay more attention to hydrogen within minerals occurring deep inside Earth, which were proposed to store an even larger amount of water than that on Earth.

It has been gradually established that the majority of the Earth's hydrogen indeed exists as structural water within crystal lattices of high-density silicate minerals in Earth's interior [1,2]. This concept mostly stemmed from results of high-pressure and temperature synthesis experiments on a wide variety of high-density minerals, which were often ≤100 μm in their crystal sizes. After detailed structure analysis using intense X-ray and neutron beams, which were only available at large-scale experimental facilities, the concept has been continuously reinforced. On the other hand, laboratory-based X-ray diffraction analysis also suggested that hydrogen concentration could be evaluated independently and quantitatively from accurate structure parameters of minerals once these parameters were successfully determined [3]. Thus, in this study, we aim to determine the structure parameters of these synthetic mineral crystals at such small sizes using a micro-focused X-ray diffraction scheme that is available at KURNS.

EXPERIMENTS and RESULTS: In order to evaluate how accurately the lattice parameters can be determined using the micro-focused beam of 100 μm, a systematic analysis of already well-characterized standard samples with varying crystal sizes is needed first. For the first year of the project, therefore, we evaluated the lattice parameter of pure aluminum powder with different grain sizes. Figure 1 shows representative results obtained using CuKα X-ray focusing optics of Rigaku SmartLab 9 kW, which provide implications for how the effects of grain size and diffraction angle are quantitatively corrected. It was proven that there is no effect of the grain size on 2θ and an angle-independent effect on it. These results were essential for obtaining precise lattice parameters for the actual mineral samples [4].

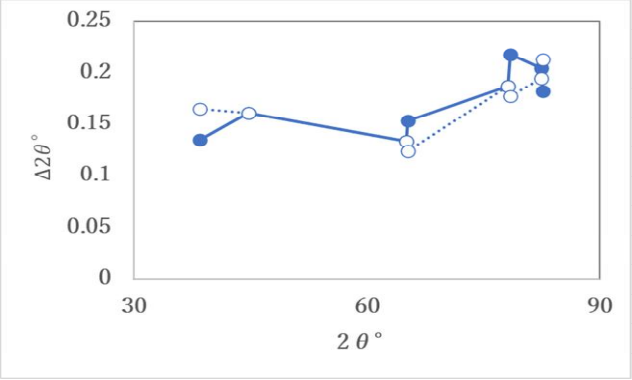

Fig. 1. Systematic diffraction angle error (Δ2θ) as a function of 2θ, which was evaluated from micro-focused X-ray diffraction patterns of pure aluminum powder sample of 45 μm (open circle) and of 3 μm (solid circles).

REERENCES:

[1] S. Karato, Earth Planet. Sci. Lett., **301** (2011) 413.
[2] N. Purevjav et al., Am. Mineral., **109** (2024) 1036.
[3] J. R. Smyth *et al.*, Geophys. Res. Lett., **33** (2006) L153011.
[4] N. Tomioka et al., KURNS Progress Report (2026) R7015.

ACKNOWLEDGMENTS:

We thank C. Umehara for his support for experiments and data analysis.

CO5-5

Noble gases and halogens in serpentinite-related metasomatic rocks constrain time-dependent changes in the origin of aqueous fluids in the shallow mantle wedge

H. Sumino[1], K. Aida[2], S.R. Wallis[2], H. Kawamura[1], H. Yoshino[3], Y. Iinuma[3], H. Yoshinaga[3] and R. Okumura[3]

[1]*Research Center for Advanced Science and Technology, University of Tokyo*
[2]*Department of Earth and Planetary Science, University of Tokyo*
[3]*Institute for Integrated Radiation and Nuclear Science, Kyoto University*

INTRODUCTION: In the ^{40}Ar-^{39}Ar and I-Xe dating methods, radiogenic daughter isotopes (^{40}Ar and ^{129}Xe) and parent elements (potassium and iodine) are simultaneously determined by converting ^{39}K and ^{127}I to ^{39}Ar and ^{128}Xe, respectively, via neutron-induced nuclear reactions in a nuclear reactor, and by noble-gas mass spectrometry. As halogens (fluorine, chlorine, bromine, and iodine) are also converted to corresponding noble gas isotopes by neutron irradiation and detection limits for noble gas isotopes by mass spectrometry are pretty low (down to ten thousand atoms), they can also be analyzed with high sensitivity by using the same method [1].
Fluids released as plates subduct play an essential role in generating active magma and seismic activity at convergent margins. High-pressure, low-temperature metamorphic belts preserve rocks that record processes along the plate interface in subduction zones and commonly contain ultramafic units derived from the mantle wedge. These ultramafic rocks are generally surrounded by metasomatic zones composed mainly of hydrous minerals. Such metasomatic zones are direct geological records of hydrous fluids moving along the slab-mantle interface and transporting various chemical species. Neither the origin of the fluids nor the pathways followed once they are released by dehydration is well known. We investigated the origins of fluids in several ultramafic bodies and their surrounding metasomatic reaction zones in the Sambagawa metamorphic belt in Japan using noble-gas mass spectrometry on fluid inclusions and crystalline water in hydrous minerals.

EXPERIMENTS: Samples weighing 5-50 mg each and standards for neutron fluence were wrapped in aluminum foil and placed in aluminum capsules with ϕ10 mm x 30 mm. The capsules were irradiated with neutrons in KUR. After the irradiation, the samples were sent to the University of Tokyo. The samples were loaded into an ultra-high-vacuum line for noble-gas extraction, purification, and separation. Noble gases were extracted from the samples by heating up to 1800°C, purified with hot Ti-Zr getters, separated into each noble gas with temperature-controlled cold traps, and then their isotope compositions were determined with a noble gas mass spectrometer [1]. The thermal and fast neutron flux was estimated from the production of ^{39}Ar and ^{38}Ar from ^{39}K and ^{37}Cl in the Hb3gr hornblende standard, in which K and Cl contents have been determined.

RESULTS: The noble gas and halogen compositions of the metasomatic rocks revealed two distinct fluid inflow events: (1) serpentinization of the wedge mantle, in which fluids of altered oceanic crustal basalt origin caused the initial serpentinization of ultramafic bodies in many localities, indicating that dehydration of altered oceanic crustal basalts continues to be an important source of subduction fluids at depths beneath the wedge mantle, and (2) boundary rock formation (formation of talc, amphibole, and chlorite) in a range of different metasomatic lithologies showing relationships between the type of hydrous mineral and the origin of the fluid, which was heterogeneous from place to place and may have changed with time [2].

REFERENCES:
[1] M. Kobayashi, *et al.*, Chem. Geol., **582** (2021) 120420.
[2] K. Aida, S.R. Wallis, H. Sumino, and M. Yokota, Lithos 524-525 (2026) 108400.

CO5-6

Ar-Ar dating of single mineral grains from heavily-shocked chondrites

R. Okazaki[1], Y. Tobimatsu[1] and M. Inagaki[2]

[1]*Department of Earth and Planetary Sciences, Kyushu University*
[2]*Research Reactor Institute, Kyoto University*

INTRODUCTION: Collisions between celestial bodies in space have occurred repeatedly on various scales from the formation of the solar system to the present day. The temperature and pressure increases caused by collisions vary significantly in both time and space. Quantitatively evaluating these physical parameters allows us to extract information about individual collision events. Timing and physicochemical conditions of collisional events could be recorded in Ar-Ar ages of meteorites due to the high volatility of Ar.

We have developed Ar-Ar dating for samples of sub-milligram mass (e.g., Projects #R3007, R3038, R3127, and R5006). Through previous collaborative research, it became possible to perform Ar-Ar dating with approximately seven temperature extraction steps even on a plagioclase grain of <0.1 mg. During the proposed research period, we aimed to achieve gas extraction and dating with more detailed temperature steps, approximately 10-15 steps, to obtain physical conditions during shock-induced heating.

EXPERIMENTS: In this study, we have isolated plagioclase grains from a heavily-shocked (shock stage 5) L6 chondrite, Northwest Africa (NWA) 7984. Grains of orthoclase [1], wollastonite, and sanidine were used as the standard samples. The meteorite samples and our standard samples were placed in a conical dimple (φ1, depth ~ 0.5 mm) of a sapphire disk (φ5.5, 1.5 mm thick), and covered with a sapphire disk (φ5.5, 0.3 mm thick). Each of the sapphire container was wrapped with pure aluminum foil. These Al-wrapped containers were stacked and sealed in the capsules for the Hydro irradiation. The sample irradiation was conducted in November 2025 under our nominal condition (1MW × 46 hours + 5MW × 6 hours). The irradiated samples were recovered and transported to Kyushu Univ. in December after the decays of short-lived nuclides.

RESULTS: Our original plan was to conduct Ar isotope analysis in March 2026. However, due to repeated failures of the noble gas mass spectrometer, the analysis scheduled is postponed. The irradiated samples have been preserved, and we plan to conduct noble gas isotope analysis as soon as possible after the repair of the mass spectrometer is completed.

REFERENCES:

[1] S. Weiss, Mineralien Magasin Lapis. **16** (1991) 13–14.

CO5-7

Absorption of alkali metal ions by white radish sprouts (VII)

M. Yanaga[1], T. Kirino[2], Y. Kusumoto[2], K. Tsubouchi[2], H. Yoshinaga[2], R. Okumura[3] and Y. Iinuma[3]

[1]*Center for Radioscience Education and Research, Faculty of Science, Shizuoka University*
[2]*Department of Chemistry, Faculty of Science, Shizuoka University*
[3]*Institute for Integrated Radiation and Nuclear Science, Kyoto University*

INTRODUCTION: ^{137}Cs, released by the Fukushima Daiichi nuclear power plant accident in March 2011, has a long half-life and remains in agricultural soils, causing the harmful rumors. Our previous research has shown the possibility of extracting radioactive cesium through ion exchange decontamination using alkali metal ions [1, 2]. However, the rubidium and cesium ions used in decontamination may affect plant growth. Therefore, we aimed to clarify how alkali metal elements affect the absorption and distribution of inorganic elements by plants by cultivating radish sprouts under different concentration conditions of rubidium nitrate and cesium nitrate and measuring the content of trace elements present in the leaves and stems by activation analysis.

EXPERIMENTS: Aqueous solutions of cesium nitrate and rubidium nitrate at concentrations of 10^{-3} mol/L, 10^{-4} mol/L, and 10^{-5} mol/L, respectively, were prepared and added to germinated radish sprouts. Four samples of each concentration were cultivated, harvested after 10 days, and separated into leaves and stems. After drying, the trace elements contained in each were quantified by instrumental neutron activation analysis.

The samples in polyethylene capsules were irradiated in Pn-3 for 90 seconds. As comparative standards, the certified NIST Standard Reference Ma-te-rial 1577b Bovine Liver as well as elemental standard for Mg was used. The ν-ray spectroscopic measurements with an HPGe detector were performed repeatedly: the first measurements for 120 – 150 seconds after decay time of 5 - 15 minutes and the second one for 250 - 300 seconds after 60 - 150 minutes.

RESULTS: When comparing the manganese concentrations in the group treated with rubidium nitrate and the group treated with cesium nitrate, the concentration was lower in the group treated with cesium. Since manganese is an element involved in plant photosynthesis, it is thought that the absorption of manganese was inhibited by the addition of cesium, which may have caused the growth disorders.

Next, we will discuss alkali metal concentrations. First, in both the rubidium-added group and the cesium-added group, the potassium concentration decreased as the concentration of the added solution increased. This suggests that the absorption of rubidium and cesium ions is competing with the absorption of potassium ions. On the other hand, the sodium concentration was significantly higher in the cesium-added group compared to the rubidium-added group. Furthermore, no concentration dependence was observed in either group. This suggests that even within the same alkali metal group, the way sodium is absorbed differs between plants treated with cesium and those treated with rubidium.

Considering the decrease in manganese concentration in radish sprouts and the differences in sodium absorption in the cesium-added group, as well as the use of fields after decontamination, it is considered that rubidium is better than cesium for decontaminating radioactive cesium from soil.

REFERENCES:

[1] M. Yanaga et al., NMCC ANNUAL REPORT, 22 (2015) 185-190.
[2] M. Yanaga et al., NMCC ANNUAL REPORT, 23 (2016) 172-179.

CO5-8

Determination of Abundance of Rare Metal Elements in Seafloor Hydrothermal Ore Deposits by INAA Techniques-12: Determination of Barium in Sulfide-sulfate Ore (2)

J. Ishibashi[1], J. Goto[2], R. Kinugasa[3] S. Toyoda[3], H. Yoshinaga[4], Y. Iinuma[4] and K. Takamiya[4]

[1] *Kobe Ocean-bottom Exploration Center, Kobe University*
[2] *Faculty of Ocean Science and Technology, Kobe University*
[3] *Department of Applied Physics, Okayama University of Science*
[4] *Institute for Integrated Radiation and Nuclear Science, Kyoto University*

INTRODUCTION: We have studied application of INAA technique to quick search for elemental abundance in mineralized samples collected from seafloor hydrothermal deposits. Barite ($BaSO_4$ as chemical formula) is one of important gangue minerals in such deposits, and Ba content of sulfide-sulfate ores widely varies from a few hundred ppm to more than 50 wt%. Determination of Ba content of sulfide-sulfate ores using conventional ICP-QMS analysis often provides poor results due to incomplete dissolution of ores during the chemical treatment [1]. We tried determination of Ba content using XRF technique, which allows for rapid analysis through a simple procedure. Here, we report a result of crosscheck analysis between INAA technique and XRF technique.

EXPERIMENTS: Sulfide-sulfate ores collected from an active seafloor hydrothermal field in a sea-mount in Izu-Bonin Arc were provided for the crosscheck analysis. Aliquots for INAA and XRF analysis were split from the same powdered sample. For INAA, the samples of 10-20 mg were irradiated at Pn-3 (thermal neutron flux = 4.68×10^{12} n/cm^2/sec) for 30 seconds and the gamma ray activity was measured for 3 minutes after adequate cooling time (2-5 minutes). The peak at 661.66 keV of Ba-137m (t½=2.552 minutes) was used for quantification. The Ba content in the samples was calculated based on relative comparison of peak areas with a pure barite crystal grain collected from the Kosaka mine. XRF analysis was performed in CSREA, Kobe University, using the energy-dispersive XRF analyzer EA1400 (Hitachi High-Tech). Samples for measurement were prepared according to the loose power method. Determination of 10 elements (Mg, Al, Si, S, K, Ca, Fe, Cu, Zn, As, Pb and Ba) was carried out by switching the voltage applied to the X-ray tube between 15 kV and 50 kV, and by selecting appropriate filters. The Ba content was calculated from the X-ray intensity using the FP method, and a correction was applied for the oxygen content which cannot be detected by XRF.

RESULTS: The results of crosscheck analysis for the Ba content was illustrated in Fig. 1. Contents determined by two analytical techniques generally showed good agreement. However, there was a tendency for the XRF measurements to yield higher values for some samples.

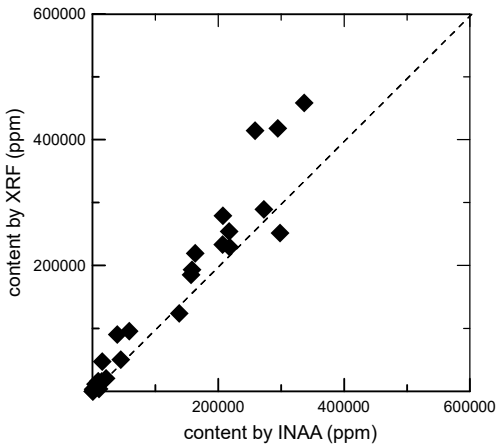

Fig. 1. Result of cross check analyses between INAA and XRF for sulfide-sulfate ores

REFERENCES:

[1] J. Ishibashi et al., KURNS PROGRESS REPORT (2021) p.152.

CO5-9

Fundamental Study on the Migration Behavior of Trace Elements from the Environment into Structural Materials Using INAA

I. Sato[1], S. Miyakawa [1], S. Okano [1], K. Sato[1], K. Onda[1], N. Kurihara[1], T. Uchiyama[1], N. Hagura[1]

[1] *Tokyo City University*

INTRODUCTION: In Fukushima Daiichi Nuclear Power Plants, various contaminated material had been generated by the severe accidents, especially concrete materials, used as structure materials, experience various conditions such as dipped into contaminated water, stayed under high temperature areas and so on. Therefore, radioactive nuclei, Cs-137 and Cs-134 had been taken in the concrete materials by penetration via solution and/or its melting, and then large amount complicated radioactive wastes were generated [1].
The complexity of contamination into the concrete materials could be related to its micro structure. In this study, the relationship of the penetration behavior and the microstructure was investigated with observation of the micro structure using X-ray and with penetration of Cs into them using INAA.

EXPERIMENTS: Mortar samples (ordinary Portland cements, W/C=0.25 and 0.55, size: 15 mm ×15 mm ×15 mm) were used in the experiments. Acrylic resin was applied to 5 of the 6 surfaces to permit penetration to one surface. The specimens were dipped into 0.01 M CsOH solution for Cs to penetration into themselves for 18 days. Then, dried specimens were grided by a thickness of 0.5 mm 4 times to make powder for INAA of KUR. On the other hand, these specimen transparency images were taken with a X-ray generator (10 keV) and a X-ray image intensifier (Toshiba E5877CS-PIK).

RESULTS: As shown in Fig. 1, in the higher W/C ratio specimen the Cs concentration was higher, which means it is easier for Cs to penetrate into high W/C concrete. Fig.2 shows the transparency images, there are more black spots in W/C=0.55 than W/C=0.25. This black spots are sparse concrete material positions, which might be passes for water containing Cs. From these results, the relationship of the penetration behavior and the microstructure was understood.

REFERENCES:

[1] K. Yamada et al, “Attempts to estimate the amount of contamination by Cs and Sr in cracked concrete considering realistic contamination conditions”, Proceedings of Waste Management Symposia 2024 (WM2024), Phoenix, (2024).

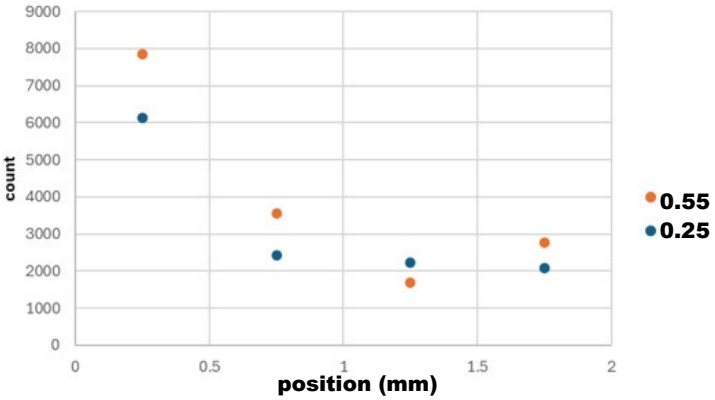

Fig. 1. Cs penetration profiles into concrete specimens (C/W=0.25 and 0.55)

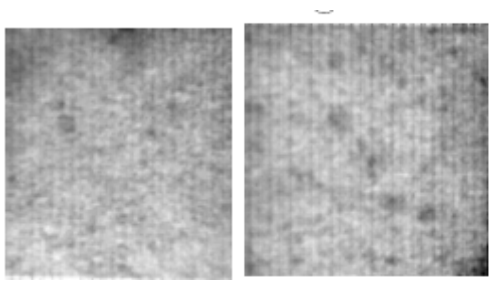

Fig. 2. Transparency images (C/W=0.25 (left) and 0.55 (right))

CO5-10

Shock deformation and structural evolution of minerals at planetary impact conditions

Y. Umeda[1, 2], T. Sekine[3], Y. Seto[4], N. Tomioka[5], and T. Okuchi[1, 2]

[1]*Institute for Integrated Radiation and Nuclear Science, Kyoto University*
[2]*Graduate School of Engineering, Kyoto University*
[3]*Center for High Pressure Science and Technology Advanced Research*
[4]*Graduate School of Science, Osaka Metropolitan University*
[5]*Kochi Institute for Core Sample Research, Institute for Earth and Material Sciences, Japan Agency for Marine-Earth Science and Technology*

INTRODUCTION: Water has played fundamental roles in the evolution of Earth and in the history of organic matter and life. Hydrous asteroids, including C-type asteroids, contain abundant hydrous minerals that store structural water mainly as hydroxyl (OH) groups. Shock-induced dehydration during high-velocity impacts may have reduced the amount of water ultimately delivered to the Earth's oceans and atmosphere. Serpentine, one of the most common hydrous minerals in these asteroids, contains more than 10 wt% structural water. Therefore, understanding the behavior of serpentine under high-velocity impact conditions is essential for evaluating the mechanisms of water transport, retention, and redistribution on the Earth.

In this study, we applied in situ ultrafast X-ray diffraction (XRD) measurements during shock compression to antigorite, a common serpentine mineral, for the first time. Shock pressures up to 106 GPa, corresponding to impact velocities of approximately 8 km/s, were generated to directly observe the structural evolution of serpentine under impact conditions. This year, we mainly focused on analyzing in situ XRD data from shock-compressed antigorite to clarify its structural evolution under high-velocity impact conditions.

EXPERIMENTS: Laser shock-compression experiments coupled with in situ XRD measurements were performed at BL3-EH5 of the SPring-8 Angstrom Compact Free-Electron Laser (SACLA) facility [1]. We prepare a fully dense single-crystal antigorite as the starting material. The target consisted of a polypropylene ablator with a thickness of 50 ± 1 μm and an antigorite layer with a thickness of 50 ± 1 μm. The XFEL pulse (λ = 1.13 Å) was focused to ~10 μm vertically and 30 μm horizontally at a depth of 25 μm within the antigorite sample. The time evolution of antigorite structure under shock compression and subsequent decompression was measured using an XFEL. The recorded two-dimensional diffraction patterns were analyzed using ReciPro software [2]. The arrival time of the shock front at the rear surface of the antigorite sample was determined using a velocity interferometer system for any reflector [1]. The average shock velocity was calculated based on the sample thickness and the measured shock transit time to estimate the shock pressure.

RESULTS: The in situ XRD results showed that shock-compressed antigorite remained crystalline up to 44 GPa, corresponding to an impact velocity of ~4.7 km/s, whereas it transformed into an amorphous state above 66 GPa, corresponding to an impact velocity of ~6.4 km/s. This transformation was completed within a few nanoseconds during the compression stage, and no recrystallization from the amorphous state was observed during subsequent decompression. These observations indicate that shock-induced amorphization is the dominant structural response of antigorite under high-velocity impact conditions. The present results provide important constraints on the collisional history and water-retention processes of hydrous asteroids such as Ryugu and Bennu. In the future of this research, we plan to conduct shock-recovery experiments using a two-stage gas gun to investigate the shock deformation and water behavior of the post-shock samples in detail.

REFERENCES:

[1] Y. Umeda *et al.*, Physics and Chemistry of Minerals, 52 (2025).
[2] Y. Seto & M. Ohtsuka, Journal of Applied Crystallography, 55 (2022).

CO5-11

Development of ^{40}Ar-^{39}Ar Dating Equipment in KURNS, Kyoto University

N. Iwata[1], Y.N. Miura[2] and M. Inagaki[3]

[1] *Faculty of Science, Yamagata University*
[2] *Earthquake Research Institute, University of Tokyo*
[3] *Institute for Integrated Radiation and Nuclear Science, Kyoto University*

INTRODUCTION: Radiometric dating is an important technique for elucidating the formation and evolution history of terrestrial and planetary materials. The K-Ar and ^{40}Ar-^{39}Ar methods are invaluable for determining the timing of volcanic eruptions, estimating cooling processes in plutonic rocks, and resolving the timing of heating events on planetesimals and asteroids (e.g., Fernandes, 2024 [1]). The ^{40}Ar-^{39}Ar dating method with the laser-heating technique is suitable for small samples (e.g., Kelley, 1995 [2] and Hyodo, 2008 [3]). To obtain ^{40}Ar-^{39}Ar dates on rock and mineral samples from terrestrial and extraterrestrial materials using the facility in KURNS, we have continued developing a ^{40}Ar-^{39}Ar dating system that includes laser-heating gas extraction and gas purification lines. The system was initially designed by Dr. R. Okazaki (Kyushu University) and has been developed for several years. Previous progress reports have described the system's details and schematic diagram (Nos. 31126, R2079, R3121, R4068, R5122, R6057).

EXPERIMENTS: To extract gas from the small sample, we prepared and adjusted a continuous-wave Nd:YAG laser (LEE Laser model 812TQ), which was installed in 2019 at KURNS. It had a continuous-wave power output of 57 W at the time of installation. However, no laser power output was observed in the latest operation test in March 2025. In FY2025, we again checked the Nd:YAG laser's current condition.

RESULTS: We confirmed that the Nd:YAG laser was malfunctioning. Then we begin considering the replacement of the laser equipment in the KURNS. One possible plan is borrowing a continuous-wave fiber laser (Wuhan Raycus Fiber Laser Technology, RFL-C300) available in KURNS, which has a ~300 W of power output and a 3 mm beam diameter. However, we are concerned that the laser's power output is too high for fusing small rock and mineral samples. Because gradual heating by controlling the laser power from low to high for extracting sample gas stepwisely is desirable for ^{40}Ar-^{39}Ar dating (e.g. [4], [5]). Another possible plan involves relocating with a diode laser (Spectra Diode Labs., FL20), which has a ~15 W output and a 7.7 mm beam diameter, from Yamagata University. We will continue considering these and other alternatives from several points of view.

REFERENCES:

[1] V. S. Fernandes, R. Burgess and H. Sumino (2024), in Methods and applications of Geochronology, edited by Shellnutt, Denyszyn and Suga, (Elsevier, 2024) 297-343.
[2] S. P. Kelley, in Microprobe techniques in the earth sciences, edited by Potts, Bowles, Reed, Cave (Chapman & Hall, London, 1995) 327-358.
[3] H. Hyodo, Gondwana Res. **14** (2008) 609-616.
[4] C. Merrihue and G. Turner, Jour. Geophys. Res. **71** (1966) 2852-2857.
[5] I. McDougall and T. M. Harrison, Geochronology and Thermochronology by the ^{40}Ar/^{39}Ar Method, 2nd ed., (Oxford Univ. Press, 1999) 269 p.

CO5-12

Observation of ^{137}Cs in tree ring of cedar from 2014 to 2025

T. Ohta[1], Y. Kashiwaba[2], K. Shinozaki[2], K. Miyazaki[2], S. Fukutani[3], Y. Shibahara[3], J. Oshima[4], T. Kubota[5], and Y. Mahara[6]

[1] *Institute of GIGAKU, Nagaoka University of Technology*
[2] *Graduate School of Engineering, Nagaoka University of Technology*
[3] *Institute for Integrated Radiation and Nuclear Science, Kyoto University*
[4] *University Forests, Faculty of Agriculture,Utsunomiya University*
[5] *Agency for Health, Safety and Environment, Kyoto University*
[6] *Kyoto University*

INTRODUCTION: Vast forest was markedly contaminated by radioactive plums containing radionuclides especially radiocesium in the wide range of the eastern part of Japan in 2011 [1–8]. As forests have an important role in preventing landslides and maintaining the ecological and hydrological system, the destructive forest should be avoided and an appropriately managed tree-felling should be conducted. In our previous field study [1], most of the radiocesium in the tree rings was directly absorbed by the atmospheric direct uptake via the bark and leaves rather than by roots. We collected cedar samples from 2014 to 2025 and determined radiocesium in annual tree rings of cedar observed at Utsunomiya University Forestry Center.

EXPERIMENTS: The cedar were cut and dried in an oven. They were then packed into U8 containers to create uniform sources for gamma ray measurements. The radioactivity intensity within the samples was measured using a high-purity Ge semiconductor detector (SEIKO EG&G). To quantify the radioactivity intensity of the radionuclides, the peak energy of the gamma rays was used, specifically 662 keV for ^{137}Cs. The detailed measurement methods are described in Ohta et al. [6]

RESULTS: The ^{137}Cs concentration in the annual tree rings of cedar trees did not increase during 2014 - 2025. In cedar trees sampled 3.8 months after the Fukushima accident, the concentration of radioactive cesium in the aboveground sapwood was slightly greater than that in the heartwood. In the Nishiyama area of Nagasaki, where black rain from the atomic bomb is thought to have fallen, the ^{137}Cs concentrations in the annual tree rings of cedar trees were higher in heartwood than in sapwood [8-10]. The annual tree rings of the aboveground parts of the Utsunomiya cedar trees are likely to show increased accumulation of radioactive cesium in the heartwood, similar to the data from the cedar trees observed by Nagasaki [8-10].

REFERENCES:

[1] Y. Mahara *et al.*, Sci. Rep., **4** (2014) 7121.
[2] T. Ohta *et al*., J. Radioanal. Nucl. Chem., **310** (2016) 109-115.
[3] Y. Mahara *et al.*, Sci. Rep., **11** (2021) 8404.
[4] T. Ohta *et al*., Radiological Issues for Fukushima's Revitalized Future, Ed Takahasi (Springer) (2016) 13-24.
[5] T. Ohta *et al*., Ana. Sci., **29** (2014) 941-947.
[6] T. Ohta *et al*., J. Environ. Radioact., **111** (2012) 38-41.
[7] T. Ohta et al., Sci. Rep., **13** (2023).
[8] Kudo et al., J. Environ. Radioact., **21** (1993) 55–63.
[9] Garrec et al., Appl Radiat Isot., **46** (1995) 1271–1278.
[10] Mahara and Kudo, Appl Radiat Iso., **46** (1995) 1191-1201.

CO5-13

Development of Neutron Detection System for Lunar Water Resource Exploration

T. Fujiie[1], T. Enoto[2], M. Numazawa[3], N. Tsuji[2] and M. Tsurumi[2]

[1] *Department of Physics, Konan University*
[2] *Department of Physics, Kyoto University*
[3] *Department of Physics, Tokyo Metropolitan University*

INTRODUCTION: This study aims at the fundamental development of a neutron detection system for a lunar orbiter to investigate the distribution of water resources on the Moon through measurements of lunar-origin neutrons. The presence of water has been suggested in permanently shadowed regions such as the lunar poles and craters. The presence of water on the Moon serves to slow down high-energy neutrons generated by the interaction between galactic cosmic rays and the lunar surface, converting them into thermal neutrons. In other words, observing thermal neutrons originating from the lunar surface using a lunar orbiter can enable the exploration of water resources on the Moon. To enable deployment on a satellite platform, we develop a compact, lightweight neutron detector with a high signal-to-noise ratio, together with a focusing system. The performance of the system is evaluated through ground-based experiments using thermal neutron irradiation.

EXPERIMENTS: As the first step in developing a neutron detection system for satellite deployment, we have developed a neutron detector that combines a plastic scintillator (EJ-270) with a semiconductor photodetector (SiPM). The neutron detector was installed on the sample stage of the CN-3 beamline[1], and the thermal neutrons collimated to 10 × 1 mm were sequentially irradiated onto multiple locations on the detector surface. The observed signals were identified as neutrons and others using pulse shape separation (PSD) techniques.

RESULTS: Figure 1 shows the signal height, PSD value, and count rate observed when neutrons were irradiated onto the detector. This figure indicates that two types of signals with different PSD values and pulse heights were observed. The intensity of the neutron-induced signal was about 70 cps. These results indicate that the neutron detector we developed is functioning properly with respect to thermal neutrons. While the discrimination capability did not vary significantly depending on the irradiation position, the number of detected neutrons showed a maximum variation of 10% relative to the irradiation position. To investigate the cause of this, we plan to evaluate the irradiation position dependence in greater detail and modify the PSD conditions.

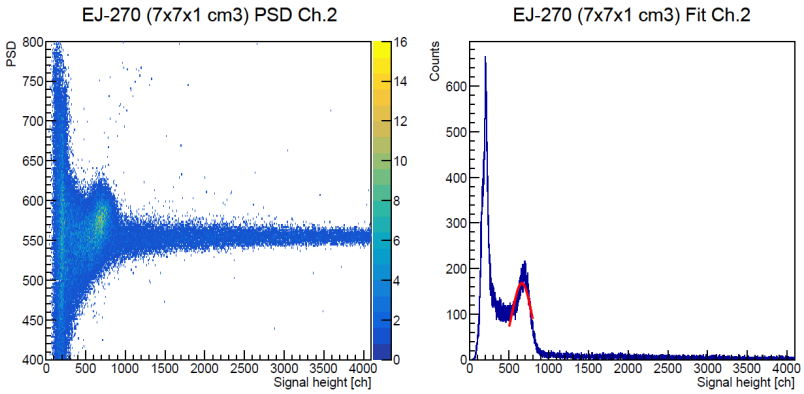

Figure 1. (Left) The relationship between the observed signal height, PSD value, and count, and (right) its projection.

CO5-14

Interaction of molybdate with calcium in saline water

T. Kubota[1], N. Abe[2], T. Takahashi[2], Y. Shibahara[2], and S. Fukutani[2]

[1]*Agency for Health, Safety and Environment, Kyoto University*
[2]*Institute for Integrated Radiation and Nuclear Science, Kyoto University*

INTRODUCTION: Molybdenum is a very important element for industry and present in trace amounts in seawater. The recovery of molybdenum in seawater requires a preconcentration step from a large amount of seawater using inexpensive and environmentally friendly reagents. Calcium chloride, which is easily acquired from seawater, was selected in this study. We have investigated the coprecipitation of molybdenum with calcium salts in saline water using radioactive tracers, molybdenum-99.

EXPERIMENTS: Molybdenum-99 was produced using natural isotopic molybdenum through photo nuclear reaction at the KURNS linac [1]. The powder of MoO_3 irradiated above was dissolved with a small amount of 0.1 M NaOH and diluted to prepare a stock solution of molybdenum. A small amount of the stock solution was diluted with 0.5 M NaCl to prepare an initial solution with a molybdenum concentration of 10^{-5} M and then was added with $CaCl_2$, $NaHCO_3$, and NaOH to induce the precipitation of calcium salts. Molybdenum was recovered by co-precipitating with the calcium salts. Its recovery ratio was calculated based on the total radioactivity and the resulting radioactivity in the aqueous phase.

RESULTS: The molybdenum recovery ratio depended on the concentration of coexisting calcium. The recovery ratio increases significantly when the calcium concentration exceeded 1.5 M in Figure 1. The variation in the data points in the figure might show that factors other than calcium concentration affect the molybdenum recovery ratio. As shown in Figure 2, the molybdenum recovery ratio is significantly affected by pH, particularly when the calcium concentration exceeds 1.5 M. Regardless of the calcium concentration, the recovery ratio was almost constant between pH 6 and pH 11. Conversely, when the pH exceeded 11.8, the recovery ratio decreased.

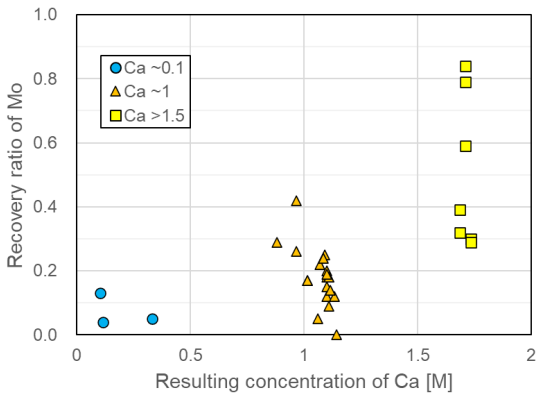

Fig. 1. Recovery ratio of Mo as a function of the resulting concentration of Ca

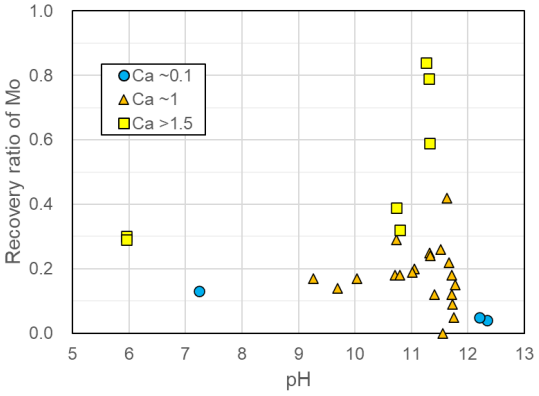

Fig. 2. Recovery ratio of Mo as a function of pH

REFERENCES:

[1] T. Kubota *et al.*, KURNS Progress Report 2019 (2020) 31110.

CO5-15

Three halogens (Cr, Br and I) in Qiquanhu eucrite

N. Shirai[1], M. Ebihara[2] and M. Inagaki[3]

[1] *Faculty of Science, Kanagawa University*
[2] *Department of Chemistry, Tokyo Metropolitan University*
[3] *Institute for Integrated Radiation and Nuclear Science, Kyoto University*

INTRODUCTION: Eucrites are basaltic achondrites derived from the crust of the asteroid 4 Vesta. These chemical compositions provide important insights into igneous processes and volatile behavior in small planetary bodies. Halogens (Cl, Br and I) are of particular interest because they are highly incompatible and sensitive to secondary processes such as degassing and fluid interaction. However, halogen abundances in Antarctic meteorites are often elevated due to terrestrial weathering, which makes it difficult to extract primary geochemical information. To minimize such effects, Qiquanhu eucrite meteorite was selected in this study. Qiquanhu is a recent fall (847 g) recovered from Tulufan, north-central Xinjiang Uygur Autonomous Region, China, in 2021. In this study, we determined the concentrations of the three halogens (Cl, Br and I) in Qiquanhu eucrite meteorite using RNAA to discuss the degassing history of this eucrite.
EXPERIMENTS: Qiguanhu meteorite was analyzed using RNAA together within the two USGS reference samples (BCR-2 and DTS-2b) as control samples. The analytical procedure of RNAA is described in Ebihara et al. [1]. Samples were weighed into plastic vials and an appropriate amount of each halogen standard solution was dropped on a filter paper and sealed in polyethylene as halogen reference samples. Both of these were irradiated for 20 min at the Kyoto University Research Reactor Institute. Known amounts of three halogens and Mn carriers were added into a Ni crucible with the irradiated reference materials and then were fused in NaOH. The fused cake was digested in water, and a hydroxide precipitate was removed from the supernatant, which contained the halogens. After acidification of the supernatant, iodine was precipitated as PdI_2, and Cl and Br were precipitated as a mixture of AgCl and AgBr precipitates. These precipitates were subjected to the measurement of ^{128}I, ^{38}Cl, and ^{82}Br. The chemical yields of the three halogens during radiochemical separation were determined using the reactivation method. To correct the effects of neutron flux gradient and neutron attenuation, samples were sandwiched by a reference standard, which was prepared by dropping a known amount of I standard solution on a filter paper.
RESULTS: The concentrations of Cl, Br, and I in BCR-2 were 102 $\pm$ 4 ppm, 0.0875 $\pm$ 0.0068 ppm, and 0.012 $\pm$ 0.004 ppm, respectively. Those in DTS-2b were 12.3 $\pm$ 0.5 ppm, 0.0863 $\pm$ 0.0066 ppm, and 0.152 $\pm$ 0.010 ppm, respectively. Although our Br data for the two samples were lower than the literature values [1], our Cl and I data were in good agreement with these values. The concentrations of Cl, Br, and I in Qiquanhu were 46.2 $\pm$ 1.2 ppm, 0.007 $\pm$ 0.002 ppm, and 0.023 $\pm$ 0.009 ppm, respectively. The concentration ranges for fall eucrite are 5.7 – 298 ppm for Cl, 0.055 – 0.149 ppm for Br, and 0.010 – 0.048 ppm for I. Although our Cl and I data for Qiquanhu fall within these ranges, its Br value is significantly lower than the literature values [2]. Halogen elements are geochemically classified as incompatible and are generally expected to show positive correlations with other incompatible lithophile elements such as La [2]. However, previous studies [2] observed that halogens in eucrite do not correlate with incompatible lithophile elements, suggesting that their concentrations were affected by degassing during igneous processes. Compared with the literature values for eucrite, Qiquanhu exhibits overall lower halogen concentrations, with a particularly pronounced depletion of Br. This feature suggests that Qiquanhu experienced more extensive degassing than other eucrites.
REFERENCES:
[1] M. Ebihara *et al.*, Geostand. Geoanal. Res., **47** (2023) 931-944.
[2] G. Dreibus and H. Wanke. *Meteoritics,* **20** (1985) 367-S381

CO5-16

Evaluation of Cs and Sr dynamics in forest ecosystems

Y. Shimada[1], S. Kuzuno[1], K. Endo[1], M. Ikegami[1], S. Fukutani[2]

[1] *Graduate School of Engineering, Kyoto University*
[2] *Institute for Integrated Radiation and Nuclear Science, Kyoto University*

INTRODUCTION: The forests which make up about 70% of Fukushima Prefecture remain undecontaminated except for an area of about 20 m from the forest edge. In order to lower the ambient dose rate in the forests and aim for the reconstruction of lifestyles and industries that surround the forests, it is necessary to decontaminate the forests beyond 20 meters from the forest edge in a feasible manner that is appropriate to the local circumstances. The ultimate goal of this study is to evaluate the effect of decontamination on reducing ambient radiation dose within the forest and its negative impact on the forest ecosystem by constructing a model that can quantitatively evaluate the concentration of radioactive cesium in fallen leaves, roots, and soil of trees, as well as the distribution and transfer of nutrients in forest soil. In this fiscal year, we analyzed the distribution and transfer of Cs-137 concentration in vertical soil on forest slopes and in fine roots of trees in the soil as well as nitrogen in the soil.

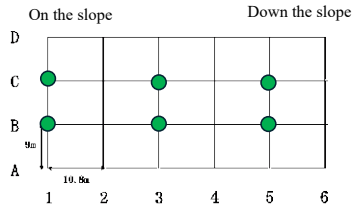

Fig. 1 Sampling points

Table 1 Inorganic nitrogen concentration in soil layers

		NH_4-N[mg/kg]	NO_3-N[mg/kg]	TN[mg/kg]
B1	Soil layer(0-5cm)	18.41	0.23	4472.81
	Soil layer(5-10cm)	5.18	2.39	1004.47
B5	Soil layer(0-5cm)	5.71	13.28	7133.05
	Soil layer(5-10cm)	7.03	0.65	5738.32
C1	Soil layer(0-5cm)	5.98	3.59	1602.55
	Soil layer(5-10cm)	8.43	1.28	2019.46
C5	Soil layer(0-5cm)	3.60	6.86	4929.02
	Soil layer(5-10cm)	3.12	5.87	4213.44

MONITORING: Litter, organic, and soil layers were collected at approximately 10m grid points (Fig.1) within a 27m x 54m area of a forest slope in Mariyama, Kawauchi Village, Fukushima Prefecture on Sep 3, 2025.

RESULTS AND DISCUSSION: Measurements of Cs-137 concentrations in the litter layer, organic layer, and soil layer revealed that the highest concentration of Cs-137 was in the organic layer, followed by the topsoil layer (0-5 cm). This indicates that the majority of Cs-137 is adsorbed in the organic layer and topsoil layer. As shown in Table 1 and Fig.2 nitrogen concentrations are higher in the surface layer (0-5 cm). Furthermore, the concentration of inorganic nitrogen is much lower than that of total nitrogen, indicating that organic nitrogen is dominant in forest soils, and that a general nitrogen cycle is occurring, similar to other forests studied in this research. Also, from Table 1, it can be seen that in the soil surface layer, the NH_4-N concentration is higher than the NO_3-N concentration at the upper part of the slope (B1, C1), while the opposite is true at the lower part of the slope (B5, C5), showing a difference in inorganic nitrogen depending on the location on the slope. The moisture content at the lower part of the slope is high at approximately 60%, and this result is a phenomenon commonly seen in forest soils under nitrogen restrictions in Japan, suggesting that the impact of disturbance due to the accident is small regarding nitrogen. As the next step, we plan to measure the concentration of Cs-137 in mycorrhizae, and build a model that can evaluate both the effectiveness of decontamination and its impact on forest ecosystems.

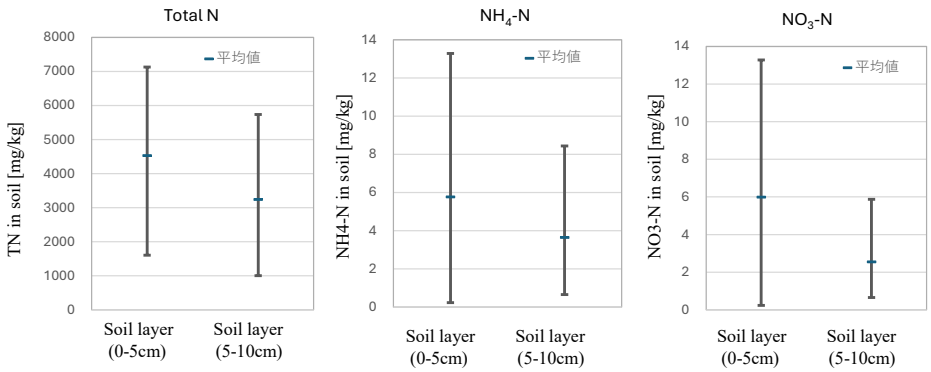

Fig.2 Nitrogen concentration measurements by soil layer

R7164

CO5-17

Fission Track Analysis of Fissile Material in Fallout Sample Collected at Maralinga in Australia

K. Takamiya, N. Osada, and Y. Igarashi

Institute for Integrated Radiation and Nuclear Science, Kyoto University

INTRODUCTION: Particles containing fissile materials are formed under conditions of high temperature and high pressure during nuclear disasters or nuclear weapon explosions. These particles can persist in the environment for extended periods. Following the Fukushima Daiichi Nuclear Power Plant accident in 2011, particles containing high concentrations of radiocesium were released and subsequently identified in environmental samples [1, 2]. Some of these particles were found to contain uranium originating from the nuclear fuel. Characterizing these particles provides essential insights for estimating the conditions within damaged reactors. Similarly, particles formed by nuclear explosions carry crucial information for reconstructing the conditions within a fireball. In a previous study, we developed a detection method for fissile substance-containing particles in environmental samples, specifically focusing on those from the Hiroshima atomic bomb [3]. This method combines fission track analysis using a research reactor. The present study aims to detect and analyze fallout particles containing fissile material in samples collected from Maralinga, Australia, one of the major atmospheric nuclear test sites.

EXPERIMENTS: Radioactive fallout particles mixed with sand were collected from the site. Initially, the particles were spread on a sheet of paper and transferred onto a paraffin film by pressing the film against the sample in a stamp-like manner. A fission track detector with dimensions of 20 mm × 20 mm was wrapped in the paraffin film to ensure direct contact between the collected particles and the detector surface. The assembly was irradiated with a thermal neutron fluence of approximately 3×10^{12} n/cm^2 using the pneumatic irradiation facility (TC-Pn) at the KUR. Following irradiation, the detector was etched in an 8 M NaOH solution at 70°C for one hour. The resulting fission tracks were then observed using an optical microscope.

RESULTS: Figure 1 shows a representative cluster of fission tracks. Similar clusters were observed in samples from Hiroshima and the Daigo Fukuryu Maru (Lucky Dragon No. 5) in our previous analyses. These clusters are consistent with those produced by fine particles containing high concentrations of enriched fissile nuclei derived from nuclear weapons. In this study, the number of tracks in each cluster ranged from several tens to a few hundreds. Furthermore, the ratio of the track density to the thermal neutron fluence for most clusters was comparable to those observed in the Hiroshima soil samples. This indicates that the particles collected at Maralinga contain fissile material at a concentration level similar to the enriched uranium-containing particles from the Hiroshima atomic bomb.

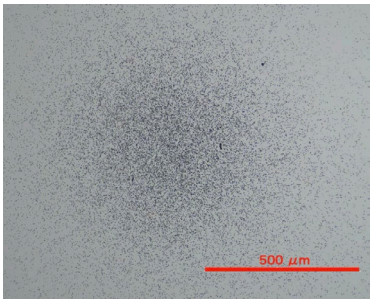

Fig. 1 Example of track-cluster formed by soil particles collected at Marcoo site in Maralinga.

However, based on the observed track distribution, the particle sizes for some clusters are estimated to be from a few to several hundred μm, which is significantly larger than those detected in Hiroshima. Since these larger particles were likely formed through a different process than the smaller ones, further investigations, including chemical analysis and SEM observation, are necessary to elucidate their formation mechanisms.

REFERENCES:

[1] K. Adachi et al., Scientific Reports, **3** (2013) 2554.
[2] Y. Satou et al., Geochemical Journal, **52** (2018) 137.
[3] K. Takamiya et al., KURNS Progress Report 2023 (2024) 163.

CO5-18

A Study on the Influence of Major Matrix Cations (Ca^{2+}, Na^{+}, K^{+}) on the Analysis of Radiostrontium in Seawater Using a Newly Developed Sr Sorbent

H. Minowa[1], Y. Ogata[2], S. Kojima[2], T. Arinobu[2], Y. Kato[3], K. Sueki[4] and S. Sugihara[5]

[1] *The Jikei University School of Medicine*
[2] *Aichi Medical University*
[3] *ALOKA Co., Ltd.*
[4] *Tokyo Metropolitan University*
[3] *Oita University*

1. INTRODUCTION: We are developing a method of rapid and safe analysis for radiostrontium in seawater for environmental monitoring. Using a newly developed strontium (Sr) sorbent, "Pureceram MAq® (Nippon Chemical Industries, Ltd.)," composed of barium silicate, it is possible to selectively sorb Sr from seawater.
This study aimed to confirm the interference from major seawater cations in the sorption of Sr, particularly calcium (Ca), which belongs to the same alkaline earth group. This study investigates the sorption behavior of Ca, sodium (Na), and potassium (K) using radioactive tracers.

2. EXPERIMENTS:
2.1 Tracer Preparation
Short-lived radionuclides were produced by neutron activation by 10sec - 30min irradiation: ^{47}Ca (half-life 4.5 d), ^{24}Na (half-life 15 h), and ^{42}K (half-life 12 h). Those irradiated reagents containing these radionuclides were dissolved to prepare tracer solutions.
2.2 Sorption Experiment
Simulated seawater (100 mL adjusted to a 0.1 M HCl) was spiked with the tracers and stirred with Pureceram MAq®. To monitor kinetics, 2 mL aliquots were sampled at 0.5, 1, 2, 3, and 4 hours. The samples were filtered, and the filtrates were measured with a Ge detector. After 4 hours, stirring was stopped, and the mixture was leave overnight to reach equilibrium. The supernatant and the Sr sorbent were separated by centrifugation to determine the radioactivity ratio. A parallel experiment used high-Ca seawater (twice of the standard concentration) to assess performance under increased interference.

3. RESULTS AND DISCUSSION: Radioactivity ratios of ^{24}Na, ^{42}K, and ^{47}Ca in the solution remained nearly 100% throughout 4 hours stirring, indicating negligible adsorption by the Sr sorbent. From the overnight samples, the residual rates of ^{24}Na, ^{42}K, and ^{47}Ca in the Sr sorbent were 0.6% or less, it confirms these elements remained in the supernatant.
However, technical limitations were noted for ^{47}Ca tracer. The ^{46}Ca (n, γ) ^{47}Ca reaction yielded low activity due to 0.004% of the natural abundance of ^{46}Ca, and the small neutron cross-section (σ = 0.7 barn). Therefore, high-precision measurements were not possible. Additionally, the simultaneous production of ^{49}Ca (half-life 8.7 min) requiring a cooling time. Future experiments should allow several days after irradiation for ^{49}Ca decay to improve ^{47}Ca detection accuracy.

4. CONCLUSION: Radioactive tracer experiments effectively track elemental behavior during sorption. The results confirm that Pureceram MAq® have high selectivity for Sr against seawater cations. This method can be effective tool for developing environmental monitoring protocols.

5. REFERENCES:
[1] Y. Ogata *et al.*, Proceedings of the 26th Workshop on Environmental Radioactivity, *KEK Proceedings 2025-2*, 140-144 (2025)